Chinese Journal of Physiology 56(5): 269-281, 2013
DOI: 10.4077/CJP.2013.BAB144

Functional Connectivity Changes during Consolidation of Inhibitory Avoidance Memory in Rats: A Manganese-Enhanced MRI Study

Ke-Hsin Chen[1], Der-Yow Chen[3], and K. C. Liang[1, 2]

[1]*Department of Psychology*
[2]*Neurobiology and Cognitive Science Center, National Taiwan University, Taipei 10617*
and
[3]*Department of Psychology, National Cheng Kung University, Tainan 70101*
Taiwan, Republic of China

Abstract

Consolidation of memory involves transfer of encoded information into a durable neural representation, but how this is transacted in the nervous system remains elusive. It has been proposed that memory consolidation is subserved by formation of a cell assembly due to coincidence of pre- and post-synaptic activity therein after learning. To capture such off-line changes, manganese-enhanced magnetic resonance imaging (MEMRI) was used to trace brain activity during the memory consolidation period. Male Wistar rats were trained on the one-trial inhibitory avoidance task and received intraventricular infusion of manganese ions shortly after training. The MEMRI taken 1 day later showed that brain areas including the prelimbic, insular and anterior piriform cortices of the learning group had significantly lower memory-related MEMRI signal than those of the control group. The functional network was revealed by correlating the MEMRI signals among regions followed by graph theoretical analysis. Learning sculpted the non-discriminative connectivity among many brain regions in the controls into a network in the trained rats with selected connectivity among regions implicated in inhibitory avoidance learning. The network could be organized into three clusters presumably subserving different functions. The results suggest that the brain prunes excessive functional connectivity in a cell assembly to consolidate new memory.

Key Words: amygdala, cell assembly, medial prefrontal cortex, memory formation

Introduction

Memory processing contains encoding, storage, and retrieval of information. Consolidation of memory, which bridges the encoding and storage processes, involves an offline transfer of the newly learned behavior into a persistent neural representation that occurs within a critical time window shortly after learning (32). However, this consolidation hypothesis awaits more evidence to reveal how the nervous system transacts the encoded information in such a process. According to a dual-trace theory of memory (18), cells located diffusely in the brain would be activated by a learning event, and the after-discharge ensuing from this event but persisting after its termination acts as the short-term memory trace. Reverberation of activity among these cells leads to coincidence of pre- and post-synaptic activation that forges a cell assembly by strengthening the connectivity among the involved units. This offline processing in a critical time window lays down the long-term memory trace for later retrieval.

This thesis has been attested by susceptibility of the newly formed memory to treatments applied shortly after training, such as electrical or biochemical stimulation of the brain (for review, see 32). While

Corresponding author: Dr. Keng-Chen Liang, Department of Psychology, National Taiwan University, Roosevelt Rd., Sec. 4, Taipei 10617, Taiwan, R.O.C. Fax: +886-2-2362-9909, E-mail: kcliang@ntu.edu.tw
Received: July 31, 2012; Revised: October 8, 2012; Accepted: November 14, 2012.
 ISSN : 0304-4920. http://www.cps.org.tw

many animal studies have revealed certain brain structures critical for memory consolidation, the complete circuitry underlying memory consolidation or so-called cell assembly noted by Hebb (18) remains elusive, because methodological difficulty prevents successful tracing of activity throughout the whole brain during the consolidation period.

In human studies, functional magnetic resonance imaging (fMRI) has been used to reveal the whole brain activity under operating a mental task by detecting the blood oxygen level-dependent (BOLD) signal change. Conversely, the resting state fMRI (rs-fMRI) could be used to delineate the offline activity ensuing after a learning event and relate the neural activation to subsequent memory recall (22, 44). The functional connectivity of a specific brain area can be calculated by the correlations of signal intensity with those of others, and the pattern of change has recently been viewed to subserve memory processing (4). However, the complexity and multiple learning trials of human memory tasks render them unsuitable for elucidating the memory consolidation process due to mixture of the processes for memory consolidation and those for encoding. Thus, although the effects of consolidation on subsequent memory retrieval were reported (14, 23), evidence on the neural substrate of consolidation process *per se* is hard to obtain.

On the other hand, how a cell assembly may alter functional connectivity among its units during memory consolidation could be well tested in rats by the inhibitory avoidance (IA) task. This task yields enduring memory by a single training trial, thus the encoding and consolidation processes would not be intermingled as in the human multi-trial learning tasks. While numerous studies have adopted this task to examine the correlative or causal brain substrates of memory consolidation (for review, see 24), few study has attempted to map out the whole circuitry underlying the IA memory by using c-Fos expression. One study of this sort has focused on delineating the neural circuit involved in expression of memory after accomplishing the consolidation stage (50), thus was unable to trace the temporal dynamics within the circuitry just as the human studies mentioned above.

Manganese-enhanced magnetic resonance image (MEMRI) combined with the IA task can resolve the above issue. MEMRI differs from fMRI by the signal depending upon the manganese (Mn^{2+}) ions accumulated in the neurons. These Mn^{2+} ions not only serve as a contrast agent by changing T1 relaxation, but also label neural activity directly with the property of entering neurons *via* voltage-gated Ca^{2+} channels (37). In addition, Mn^{2+} accumulated in the soma will be transported along the axon to the projection targets (36). Hence, neural activity will alter the signal intensity in the activated site as well as all its connected areas. Further, the *in vivo* measurement by imaging no longer requires sacrifice of the animal. By adoption of this method, a memory test can be performed later and the correlation between neural signals during the consolidation period and subsequent retention performance can be obtained. By delivering Mn^{2+} in a proper route and obtaining images at an appropriate time course (43), many studies adopted MEMRI to label prolonged neuronal activation in some interested brain regions (19, 51), or to reveal developmental plasticity change (46). Accordingly, MEMRI is apt to map out the offline activity during the period of memory consolidation.

Therefore, this study used MEMRI combined with the IA task to trace whole brain activity changes during memory consolidation. The Mn^{2+} ions were infused into cerebrospinal fluid (CSF) directly to be absorbed by brain tissues, and an initial experiment was carried out to decide the appropriate time point to acquire images. Then ten animals of which CSF can be flushed out from the implanted cannula were randomly assigned to an inhibitory avoidance learning group (IA group, n = 5) or a context control group (CC group, n = 5), both received immediate post-training infusion of Mn^{2+}. The difference in neuronal activation between the groups would be assessed by the intensity on the images of which the parameters were specifically designed for detecting manganese-enhanced signals. We further calculated the mean intensity on regions of interest (ROIs) and carried out a network analysis to map out how these functional units were composed together in the experimental and control groups.

Materials and Methods

Animals

Male Wistar rats (10 to 12-week-old, weighing 302 ± 15 grams) were used in the present study. Each rat was housed individually with free access for food and water. The housing environment was maintained on a 12 hour-light cycle (lights on: 5:30 am to 5:30 pm), and all surgery and behavioral training were performed during daytime. The experimental procedure was approved by the Institutional Animal Care and Use Committee of National Taiwan University.

Intra-Cisternal Cannula Implantation

To acquire MRI signals, the implanted materials were all MR-compatible. A polyethylene catheter (PE-20) was reformed by gently heating to create a small clutch to provide a better grip with the dental cement, and a 30-gauge stylus was inserted to prevent clogging. Then the cannula was cut to a length of 4-cm, equipped with an L-shape stainless stylus, of

which the longer side of 4.1-cm-length was inserted into the cannula. A pair of custom-made plastic screws served as an anchor at the head bone to fix the cannula firmly.

The implantation procedure was modified from a previous study (27) and performed under a surgical microscope, and all implants and instruments were well sterilized by 75% alcohol before use. Animals were food-restricted for 6 hours to prevent choking under anesthesia. Rats were anesthetized with sodium pentobarbital (50 mg/kg, dissolved in normal saline, i.p.) and kept warm during and after surgery till awake. The hair near neck was shaved before the rat being secured onto the stereotaxic apparatus, and the head was bent down with the incisor bar set at -3.0 cm. An incision was made at the midline of the neck, then the muscle and tissue was dissected bluntly till exposing the occipital bone, posterior parietal bone, and cisterna magna. Two screws were anchored at the posterior parietal bone without injuring the cerebellum. A hole on the occipital bone right above the atlanto-occipital membrane was drilled, and the pieces of skull were carefully removed to expose the transparent dura mater. Puncturing the dura mater with the aid of #5 forceps, the cannula was inserted into the cisternal space, and affixed onto the head bone firmly with dental cement. The stylus was slowly pulled out of the cannula, and the CSF was let to fill into the tube and even leak out. To prevent the CSF from flowing out of the cannula, the tip was sealed by mild heat. Finally, the muscle and skin were sutured; additional antibiotic powder was applied if needed. Rats would rest for recovery for at least 3 days, and only the rats of which the CSF can be flushed out from the cannula were recruited in the experiments.

Intra-Cisternal Infusion

Before infusion, rats were hold gently in the experimenter's arm. The infusion device contained a 28-gauge dental needle cemented to a 30 cm long PE-tube connected with a 10 μl-Hamilton microsyringe. The infusion devices were first filled with distilled water and then drug was filled but separated from water by an air bubble, which also served as a marker to monitor drug flow. To accomplish the infusion, seal of the cannula tube was cut and the needle was quickly inserted into the cannula to prevent much leaking of CSF. Ten microliters of 120 mM manganese solution ($MnCl_2 \cdot 4H_2O$, MW = 197.9, dissolved in isotonic saline) were infused at a speed of 1 μl/min, which was controlled by a microinjection pump. One minute after the infusion of manganese, a volume of 5 μl normal saline was further flushed by another infusion device to ensure all the manganese solution injected into the ventricle without backflow. Animals returned to their home cage after the infusion, and no other manipulation was applied on that day.

A Prelude Experiment on Time Course of Manganese Absorption

To know the dynamics of manganese absorption *via* CSF after intra-ventricular infusion, three animals with intra-cisternal cannula were measured repeatedly in this prelude experiment. One of the animals was used as baseline control by which no manganese solution were infused before imaging. The other two received infusion once and obtained images repeatedly at different time points. The time course between infusion and imaging for the first rat was 12 and 36 h, and for the other was 24 h, 48 h, 17 days, and 35 days. Several ROIs were selected to compare the level of signal increment at different time points, and the signal increment on each ROI was calculated by the ratio to its baseline control.

Behavioral Procedure and Performance Index

The whole experimental procedure was accomplished in six consecutive days, which contained routine handling procedures followed by the IA task training and imaging. In the first three days, rats were handled to acclimate being grasped and staying calm in the arm of the experimenter. Each animal would be housed into a transportation cage for 10 min to habituate for the transportation vibration. This procedure aided to decrease the novelty and anxiety elicited on the way to the MR center, an impact that might disturb brain activity in a short time.

After being well handled, rats were subjected to the inhibitory avoidance training procedure with each event in a single day: exploring the task apparatus, association with shock followed by post-training infusion, and retention testing after MR imaging. The apparatus of the IA task was a long alley-shape box, which was divided by a sliding door into a lit side and a dark side. On the first day each rat received three repetitive trials to explore the apparatus. A rat was placed into the lit compartment with its back toward the closed sliding door, as it turned around the experimenter opened the door and the rat soon stepped into the dark compartment. The door was closed and the rat was retrieved from the alley after 10 sec of staying in the dark side. Ten animals were randomly assigned into the inhibitory avoidance learning group (IA group, n = 5) or context control group (CC group, n = 5) in the day for fear association. Animals in the IA group received an inescapable foot shook (1 mA, 1 sec) after stepping into the dark compartment, while the CC group received the same training procedure without shock administration.

Each rat received post-training infusion of 10 µl of 120 mM manganese solution followed by 5 µl normal saline. Brain images were taken 24 h after behavioral training, and rats were transported to MR center by the cage in which they have acclimated. They were anesthetized during the imaging, and then transported back to the animal room after imaging. The memory performance was tested twice: shortly after recovery from the anesthesia and a month after the first test. The latency for rats stepping into the dark compartment was measured as the behavioral index for fear memory, and the upper limit was set at 600 sec. Since the probability distribution of this behavioral index was not a normal distribution and the sample size was small, non-parametric analysis should be more appropriate because the nature of these data. All the following analyses were performed by using non-parametric statistic methods. The Mann-Whitney U was used to compare the performance between the IA and CC groups, with the alpha value set at 0.05.

Imaging Parameters and Analyses

Images were acquired on a 7T MRI system (Bruker BioSpec, Karlshruhe, Germany) with a volume coil to transmit radiofrequency pulses and a quadrature surface coil covering the rat head to receive signal. Rats were initially anesthetized with 5% isoflurane vapored in pure oxygen with a flowing rate of 500 ml/min and then secured to the MR-compatible animal head holder. The body temperature was monitored with a rectal probe and maintained at 37 centigrade by circulating warm water in the blanket system embedded in the holder. During imaging, concentration of isoflurane was switched down to 2% with the oxygen flow of 200 ml/min, and the respiration rate was also monitored to maintain at the level about 50 breaths per min. The anatomical images with T2-weighted contrast were acquired as the location scans, by using the rapid acquisition with relaxation enhancement sequence (RARE) with TR/TE = 2742/33, 204 × 204 µm in-plane resolution, and 1 mm slice thickness. A three-dimensional MEMRI dataset of high resolution was obtained by using a low flip angle gradient-echo sequence (FLASH) with TR/TE = 21.7/3.5 ms, FA = 30, matrix size = 196 × 160 × 160, and 156 µm isotropic for spatial resolution. Four averages were used, and the total acquisition time was 40 min.

All the images were analyzed by AFNI (http://afni.nimh.nih.gov/) (11) under Linux, and the main processing steps included co-registration, voxel intensity normalization, and spatial smoothing for further statistical analyses. A rat brain which had the least amount of fat tissue on head skin was chosen as reference, and each rat brain was first spatially normalized to this reference. All spatially normalized brains were averaged to create a temporary brain template, and then the spatial normalization was accomplished again by registering each original image set to the temporary template. A final version of rat template was thus created, and this template was used for drawing ROIs and presenting results.

To compare the signal intensity across animals, it is necessary to normalize the signal intensity on each brain. A reference ROI was selected on the template, and this ROI mask would be applied to each aligned brain for calculating the mean intensity. In the time course study, the signal intensity of each voxel was normalized by being divided with the mean value of a ROI selected on the dark background. However, even the infused volume of manganese was well controlled by an infusion pump, the tiny error in infusion volume or diffusion variability was still a main concern when we compared the signal intensity between groups. A good control was to normalize the whole brain intensity to a value that reflected the basal absorption for manganese so as to rectify the possible error mentioned above. Therefore in the formal study aiming for detecting the offline activity of the cell assembly, a special reference ROI was selected in the midline of the medulla, rather than calculating the background noise. This reference ROI covered part of the reticular formation, which contained the gigantocellular reticular nucleus and medial longitudinal fasciculus (38, 45), and no direct projections between this area and brain regions involved in the IA learning. Being in the midline of the brain, the signal of medulla was less variable within the group than that of the temporalis muscle which might be influenced by aliasing artifact. Though being one of the places immersed in manganese solution quickly after infusion, the signal of medulla kept rising steadily after the time point of 24 h (data shown in results). Compared to other brain regions, this low affinity for manganese in binding to the midline structures of the medulla made it a good index to reflect basal absorption rate.

The datasets normalized for both spatial and intensity dimensions were then smoothed by using a Gaussian filter with a full width at half maximum (FWHM) of 0.3 mm. The voxels located in the olfactory bulbs, cerebellum, spinal cord, and areas out of the brain were excluded from statistical analysis. Therefore only the voxels in the cerebral cortices and subcortical structures were analyzed to compare the intensity between the IA and CC group, and the non-parametrical statistics Mann-Whitney U with uncorrected $P < 0.05$ was applied. Clusters consisting of a minimum 200 above-threshold voxels (volume = 0.76 mm^3) were considered to have significant differences between groups and were displayed as blobs.

In addition to a voxel by voxel analysis, ROI

analyses were also conducted in a priori hypothesized manner based on the IA literatures (3, 21, 25, 29). In addition to the significant clusters detected in the voxel by voxel comparison, ROIs were drawn manually on the prelimbic, anterior cingulate, and insular cortices, as well as nucleus accumbens, lateral septum, bed nucleus of stria terminalis (BNST), amygdala, dorsal hippocampus, ventral hippocampus, and ventral subiculum. The caudate-putamen ROI was selected for its role in operant conditioning, while the S1 (forelimb area) and thalamus (mainly the ventroposterior nucleus) were also included for their role in somatosensory processing during a learning event. The mean intensity of ROIs was compared by a nonparametric Kruskal-Wallis one-way analysis of variance, one-tailed, $P < 0.05$. The signal change caused by the offline activation that appeared after a learning event was calculated by the formula (IA-CC)/CC %, which IA indicates the mean intensity of the ROI in the IA group and CC indicates the mean value in the CC group.

Correlational Network Analysis

To elucidate the functional connectivity among the analyzed ROIs, inter-regional correlation matrix was conducted and color-coded by pair-wised Spearman rank order correlation. This non-parametric measure was used on purpose for not having to assume normal distribution or linear relationship of the signal intensity among regions. To visualize the interactions between ROIs, the functional network was mapped by a graph theoretical analysis (for review, see 5). In such a graph, brain regions were defined as nodes and the link between two nodes reflecting their activity correlation were defined as an edge. Thus each ROI was represented by a node, and edges were built according to the strength of interregional correlation but only those significantly differing from zero ($P < 0.05$) were counted as an edge in the network built by the Pajek software version 3.0.4 (http://pajek.imfm.si/doku.php) (2). The Kamada-Kawai algorithm was used to arrange the layout of the network. The amygdala was chosen as the center node in both networks for its critical role in modulating the IA memory based on extensive literature.

Results

Time Course between Manganese Infusion and Imaging

To reveal the dynamics of manganese absorption and distribution throughout the brain, rats receiving 10 µl manganese followed by 5 µl of saline infused into the ventricle were subjected to imaging at different time points as described in the method section. Image data were shown in Fig. 1A. Twelve hours after the manganese infusion, those regions locating adjacent to the CSF space showed enhanced signal, such as the gyri of cerebellum, dentate gyrus of hippocampus, habenula, hypothalamus, and mammillary body. The pattern for image enhancement spread from the caudal to the rostral part and from periphery to the center in the following two days. A very similar pattern of signal enhancement was noted by a previous study in which manganese was directly injected into CSF (26), so the time course revealed by our prelude experiment appeared to be reliable even though it was based only on three animals.

ROI analyses were performed on two sets of regions, one for making a general comparison and the other focusing on the areas involved in the IA learning (Fig. 1B). The ratio to the baseline control was calculated on each ROI in order to compare the level of signal increment across different times. As each data point was contributed by one animal, the trend was examined without statistical analysis. The enhancement pattern of most ROIs was rising toward a peak at 48 h, but a slight dip appeared at the time point of 36 h. This might be due to drug infusion or diffusion variability, as no dip was found for the cerebellum adjacent to the infusion site at this time point. The ROI on the mammillary body was chosen for comparison due to a consideration that it was bathed in the CSF containing high concentration of manganese. Comparing to other regions, the signal increment level of the mammillary body reached plateau in the early time point and maintained at this high level for two days. At the time point of 17 days after infusion, the signal enhancing effect was still robust in all the ROIs. It took about 35 days to wash out the manganese, except there was still some signal residue in the cerebellum and BNST.

According to the enhancement pattern of ROIs related to the IA task, a time point of 24 h was adopted in the formal experiment to delineate the neural network involved in memory consolidation. The signal of these ROIs was not markedly enhanced in 12 h after infusion, because the signal level still remained on the baseline. Yet at 48 h, the amount of manganese accumulated in these ROIs might already reach the peak, and the ceiling effect would hinder the detection of difference induced by experimental manipulation. At the time point of 24 h, those ROIs showed a moderate level of signal increment, which allowed detection of further enhancement or suppression. Without confounding by a floor or ceiling effect, any learning-induced change of activity embedded in the background of spontaneous firing would stand out. This time point was compatible with the most of the IA task paradigms in which rats were generally tested 24 h after training, and it allowed com-

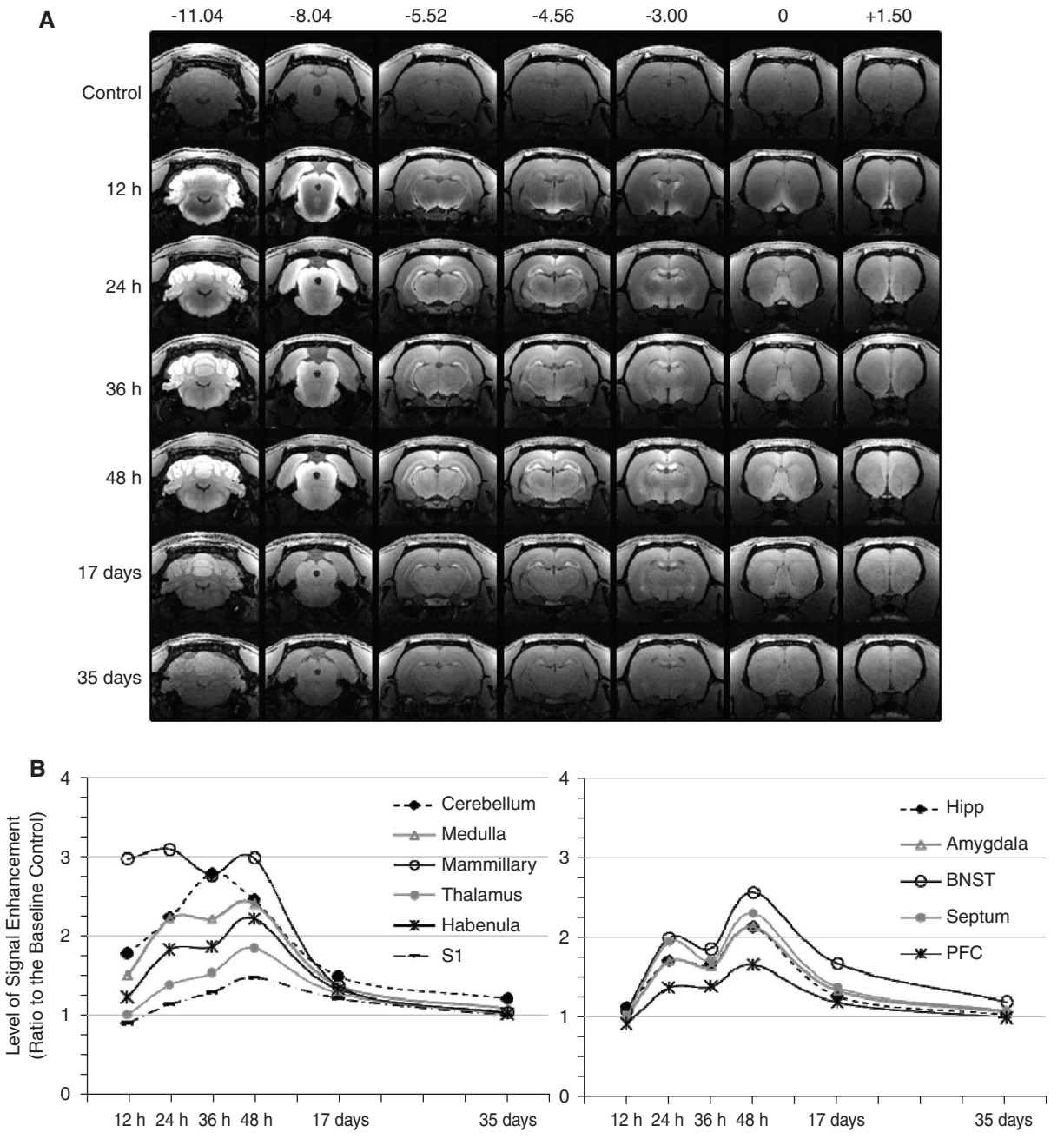

Fig. 1. The signal enhancement at various time points after manganese infusion. (A) Images acquired at different time points. The numbers placed above images denote the coordination reference to Bregma (38) in millimeter, and images were arranged caudo-rostrally from left to right. (B) The level of signal enhancement. The value on Y axis was the increment level, which was denoted the ratio to the non-manganese control. The left panel showed the overall comparison, and the right one focused on the regions involved in IA learning.

parison of our results to a vast amount of behavioral literature.

Behavioral Performance in the Inhibitory Avoidance Task

All animals survived the experimental procedure, although some animals showed less appetite and weight loss after intra-cisternal infusion. Yet these animals recovered in two days. All the animals gained weight normally (weight increment in a month: 107 ± 16 g in the IA group, 91 ± 12 g in the CC group, statistically non-significant), and no motor deficit or other abnormal behaviors were observed.

Retention performance was tested twice, *i.e.*, after MR image acquisition and a month later. Since rats in the CC group never received a foot shock in the

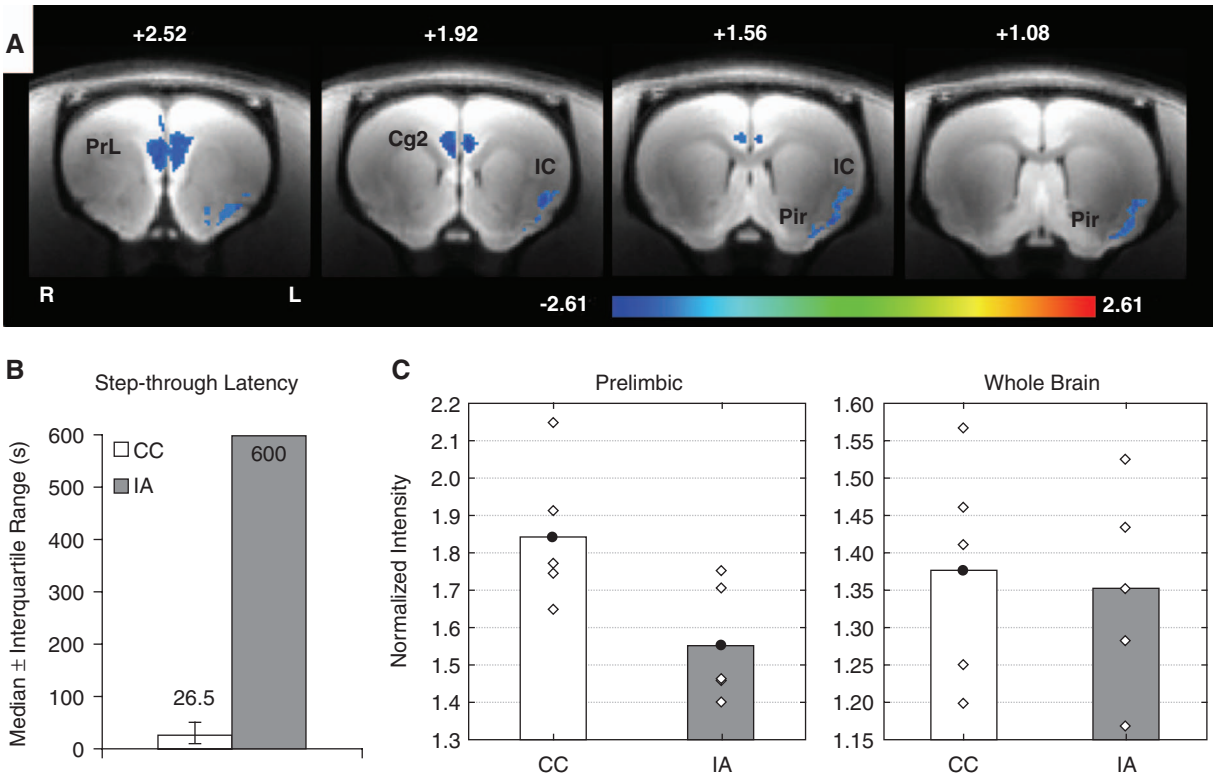

Fig. 2. The signal intensity in cortical areas showed correlates with IA memory performance. (A) Results from the whole brain analysis. Regions including the prelimbic area, cingulate cortex (Cg2), insular cortex, and anterior piriform cortex showed significantly lower intensity in the IA group (uncorrected $P < 0.05$, voxel size > 200). The row of numbers on the top indicated the coordination related to Bregma (38) in millimeter, and the color bar below brains coded for the U value. (B) Memory performance of the IA task. Significant difference in step-through latency was detected ($U = 10$, $P < 0.01$). The number shown on the bars indicates the median value. (C) The ROI analysis of prelimbic area and whole brain, respectively. The intensity of prelimbic area in the IA group was significantly reduced ($P < 0.05$), but no difference was detected in the mean intensity calculated on whole brain. The bar with close circle represents mean value; the open diamond represents the raw data. Abbreviations: PrL for prelimbic area, IC for insular cortex, pir for anterior piriform cortex, R for right hemisphere, L for left hemisphere.

dark side, the latency was significantly shorter than that of the IA group, in which rats stayed in the lit side for the whole testing period ($U = 10$, $P < 0.01$, Fig. 2B). The fear memory in the trained rats lasted for a long time, because the retention performance of the IA group remained the same in a month later (*i.e.*, all for 600 sec). This suggests that the memory trace was well consolidated and readily retrieved in either a recent or a remote memory test.

Difference in Neuronal Activity during the Consolidation Phase

To compare the signal intensity between the IA and CC groups, a group analysis was performed voxel by voxel to reveal the areas showing specific activity change in the offline processing of learned information after IA training. Fig. 2A showed that all significant blobs were located in the prefrontal region, including the prelimbic area invading into part of the anterior cingulate cortex (Cg2), insula cortex, and anterior piriform cortex. The intensity of these areas in the IA group was significantly lower than that in the CC group, for the signal change induced by offline processing in all significant voxels was -16.2% on average. The biggest blob was located at the prelimbic area, with a voxel size = 1134, signal change = -15.7% (Fig. 2C). Although several subcortical areas were better delineated than cortical areas in the image, no difference in signal intensity was detected. Moreover, no significant difference existed in the whole brain intensity (Fig. 2C), so it excluded a possibility that any difference detected was due to systematic bias *per se* rather than offline processing activity after learning.

A further ROI analyses were performed to compare the mean intensity of specific regions. Table 1 summarized the position and result for each ROI. These ROIs were selected manually, and the center of each ROI was placed at the coordinates where drug had been infused in previous studies, while that for the anterior piriform cortex was placed to enclose the

Table 1. Summary for ROI analyses

Region of Interest/Nodes (from rostral to caudal)	mean intensity		signal change	size	ROI position	edges		
	CC	IA	(IA-CC)/CC	(voxels)	(Bregma mm)	CC	IA	change
prelimbic area	1.84	1.55	-15.7%*	264	+3.00	7	1	–
anterior cingulate (Cg1+Cg2)	1.93	1.70	-11.9%#	465	+2.04	7	5	–
insular cortex	1.16	1.03	-11.0%*	246	+2.04	6	4	–
nucleus accumbens (core)	1.37	1.29	-5.2%	408	+2.04	8	3	–
anterior piriform cortex	1.18	1.07	-9.1%*	250	+1.08	0	4	+
lateral septum	1.71	1.65	-3.5%	385	+0.48	10	5	–
caudate, putamen	1.24	1.19	-3.7%	801	-0.12	10	3	–
S1 (forelimb)	1.59	1.52	-4.0%	375	-0.12	6	3	–
BNST	1.53	1.48	-2.9%	155	-0.24	9	3	–
amygdala	0.93	0.92	-1.3%	304	-3.00	10	5	–
thalamus (VP)	1.14	1.11	-2.5%	687	-3.60	9	2	–
dorsal hippocampus	1.77	1.79	1.6%	1065	-3.72	8	2	–
ventral hippocampus	1.40	1.44	2.7%	2537	-5.52	0	5	+
ventral subiculum	0.89	0.89	0.4%	153	-6.00	0	3	+
whole brain (excluding cerebellum and spinal cord)	1.38	1.35	-1.8%	300951	total edges	90	48	**

*for $P < 0.05$, # for $P = 0.07$, **$P < 0.005$, one-tailed

voxel showing lowest P value in the voxel by voxel analysis. The intensity of the prefrontal regions was significantly lower in the IA group compared to the CC group, and this result was congruent with what was shown previously. The signal of anterior cingulate cortex, of which ROI covered Cg1 and Cg2 was lower in the IA group with a signal change of -11.9% that only approached statistical significance ($P = 0.07$).

Although all the subcortical ROIs selected in the present study did not show a significant difference in signal intensity, it was found that some regions downstream to critical structures implicated in memory processing appeared to have lower signals in the IA group, for example, the lateral septum receiving the hippocampal input *via* the fornix, the BNST receiving the amygdala input *via* the stria terminalis, and the nucleus accumbens receiving convergent input from the amygdala and hippocampus. The difference between the IA and CC groups was greater in these downstream regions than that in the amygdala or hippocampus *per se*, although the difference failed to reach statistical significance.

The Functional Network of the Trained and Control Animals

Fig. 3 shows the functional connectivity among ROIs in both groups, and the value of interregional correlation was color-coded in both matrices. Each ROI was represented as a node in the functional network, and the edge was built according to the correlation coefficient that significantly differed from zero. The number of edges emitted from each node with the pattern of change after IA training was summarized in the right-most columns of Table 1. While the lateral septum and amygdala were two nodes having abundant edges connecting with other regions in both IA and CC groups, the amygdala was chosen as the graph center of each network based on its role in memory processing of the IA response. The number of edges in total or that in each ROI was fewer in the IA group, except for the anterior piriform cortex, ventral hippocampus, and ventral subiculum showing increase of edges with other nodes. Notably, these three areas did not have any functional connectivity with other areas before introduction of specific learning experience; yet they showed increased functional connectivity for selected regions when serving as nodes involving in the refined network during the memory consolidation period for the IA response.

As shown in Fig. 3A, the signal intensity among ROIs was highly correlated in the CC group, which constituted a network with plenty of interregional connections. Any two nodes within this circuitry can directly communicate. Transmission within the network lacks selectivity. On the contrary, the ROIs in the IA group could be roughly divided into three clusters showing high within-cluster correlation but low between-cluster correlation (Fig. 3B). The first cluster contained regions in the frontal lobe, where the ACC and lateral septum were the cores having most connections. The second one located at some regions in the forebrain containing caudate-putamen, S1, and

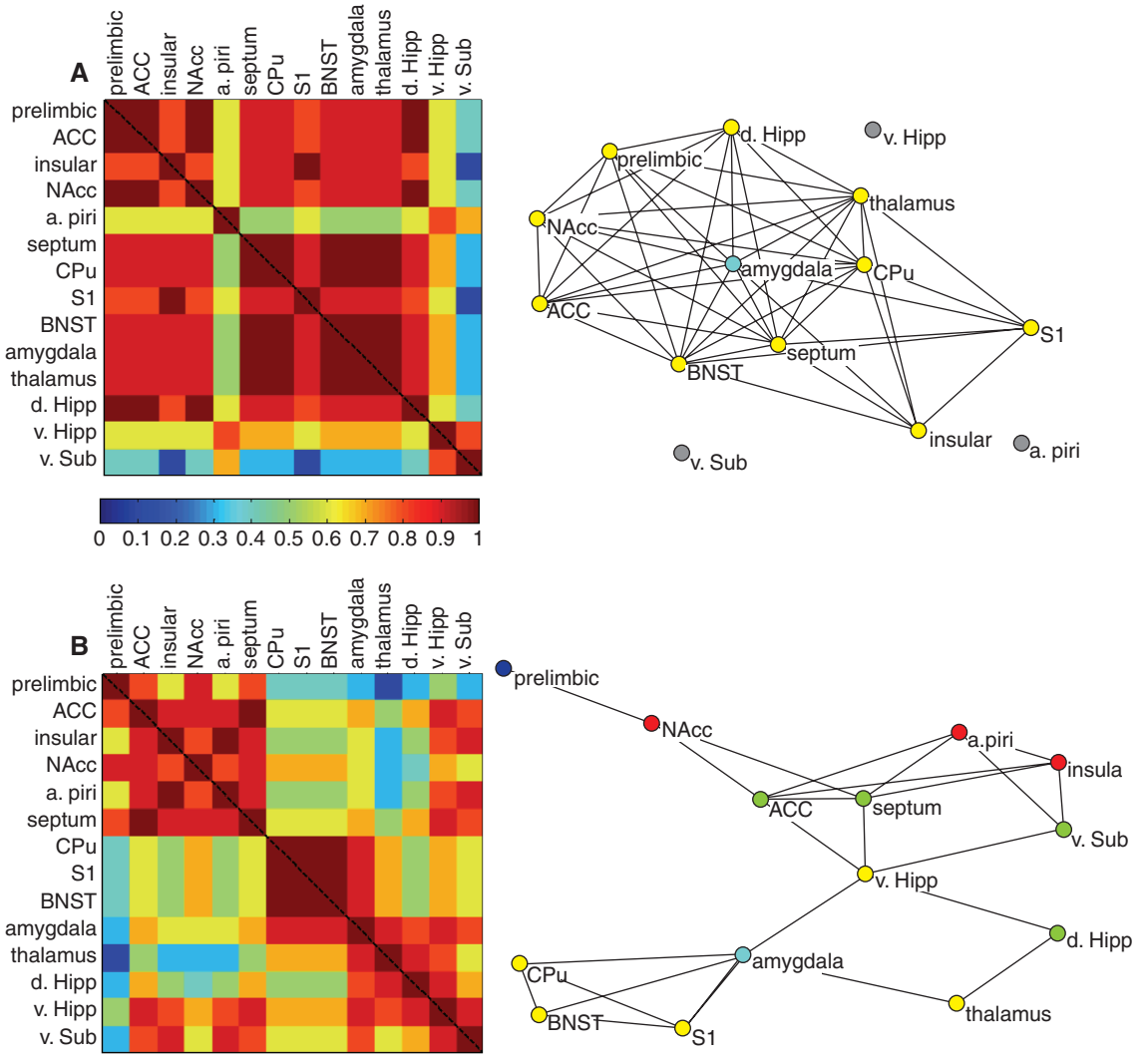

Fig. 3. The interregional correlation matrices and the functional networks. (A) The context control group. (B) The inhibitory avoidance learning group. The matrix is symmetric, and ROIs are arranged from rostral to caudal. The color in the matrix codes the value of Spearman rank order correlation. The amygdala was set as the center node of the entire network, and the color of nodes represented the steps proceeding from the center. Abbreviations: a. piri for the anterior piriform cortex, CPu for the caudate-putamen, Hipp for the hippocampus, Sub for the subiculum, d. for dorsal, v. for ventral. Color codes in functional networks: light blue as the network center (*i.e.*, amygdala), gray as no connections, yellow as one step, green as two steps, red as three steps, dark blue as four steps needed to reach the center.

BNST that were highly correlated with one another. The final cluster formed a loop including the amygdala, hippocampus, and thalamus. It is worth noting that this loop could serve as a bridge to connect the former two forebrain clusters, and the amygdala and hippocampus stood at the key position. Thus, after the functional connectivity among regions being sculpted by experience, the circuitry was reorganized into three discriminative clusters, and each of which may have different roles during the IA memory processing.

Discussion

This study used MEMRI combined with the IA task to trace the offline activity occurring within 24 h after the termination of inhibitory avoidance learning, in which contained the critical period of memory consolidation. The results showed that the activity of the prefrontal regions was significantly altered in the trained animals compared to that of the context control group. The functional connectivity was calculated among regions implicated in inhibitory avoidance learning, and a network analysis was conducted to map the relationship of the functional units. It was found that a uniformly inter-connected network was detected among the regions in the control group, and a node within the network can communicate to any other chosen nodes by direct links. In contrast, the

functional network after IA training became more discriminative and showed three clusters with very selective functional connections. These results imply that the learning experience transformed a nearly random network into a more organized one.

In the present study, MEMRI was taken to assess the neural activity related to consolidation of a recent memory within 24 h after training. MEMRI has recently been applied to trace the change of neural functions in response to various types of manipulation (10, 31, 48, 49). Previous studies have shown that consolidation of memory may involve neural processes going on in widespread brain regions including the hippocampus and amygdala within several hours after training in an awakening state or during sleep at the night after training (6, 12, 13, 17). Therefore the present study infused Mn^{2+} immediately after training and assessed the signals in various brain regions in 24 h after infusion, thus the observed signal change reflected what cumulated within a 24-h consolidation period. Because Mn^{2+} was given after the shock administration, therefore, the signal difference between the IA group and the CC group could not be attributed to reflection of shock-induced pain *per se*. As a matter of fact, application of shocks at a higher level to the limbs of rats or direct stimulation of the pain pathway increased rather than decreased activation in the cingulate regions as indicated by Mn^{2+} signal (49). Furthermore, the signal changes in the three prefrontal regions were significantly correlated with behavioral performance, suggesting the observed signal changes were indeed relevant to memory processing.

Evidence has shown that Mn^{2+} could be toxic to the nervous system at certain doses and the long entrance latencies in the IA group during the 1-day test may be due to Mn^{2+}-induced lethargy (16). This interpretation was unlikely because the good retention performance in this group was well maintained over a month later when Mn^{2+} was almost fully washed out in the brain. Additionally, rats in the CC group also received Mn^{2+} infusion but dashed into the dark compartment in either recent or remote memory tests. This observation ruled out the possibility that Mn^{2+} given after training would have affected performance. Thus, Mn^{2+} in the present study could be treated as neuronal activity tracer as well as contrast agent without disrupting memory processes.

According to postulates on memory consolidation raised by Hebb (18), learning events would launch activity reverberation within the cell assembly subserving a memory trace. This often leads to an expectation that memory consolidation would always involve increase of neuronal activity in the engaged circuitry. Indeed some studies have found long-lasting electrophysiological excitation in certain brain regions, such as the amygdala, long after a learning event (40). However, the present study found a significant decrease rather than increase of Mn^{2+} enhanced signals in several cortical regions during the 24-h consolidation period. The uniform reduction of Mn^{2+} signal could not be due to a ceiling effect as we picked a time point in which the signal baseline in the non-trained animals was at an intermediate level. This unexpected decrease of activity observed in the brain regions could be interpreted in several ways.

First, while Hebb (18) proposed reverberation of neuronal activity within a cell assembly during memory consolidation, he by no means regarded that all the neurons involved would operate in an excitation mode, which would definitely cause an ever-escalation of activity within the network and eventually escaped harness. Thus some neurons or sites must be inhibited to yield a self-contained and well-organized activity in a circuit. Some areas of the medial prefrontal cortex were shown to exert an inhibitory action of the amygdala (41), and activation of the latter structure is essential for consolidation of avoidance memory (33). Evidence showed that the medial prefrontal cortex had to be inhibited to protect consolidated fear memory from extinction (20). Indeed, certain information converging onto the prefrontal cortex involves inhibitory neurotransmission, and malfunction of this GABAergic transmission would result in behavioral abnormality or cognitive deficits. Consistently, an unconditioned fear induced by presenting the fox scent to rats would increase the MEMRI signal in the amygdala but accompanied with suppression of that in the medial prefrontal cortex (9). Of course, roles and mechanisms underlying deactivation of other brain regions such as the insular or anterior piriform cortex remain to be elucidated.

Alternatively, in the present study the Mn^{2+} signal reflected neuronal activity accumulated for a 24-h period, which contains a critical time window for memory to consolidate. Given the assumption that brain regions underlying memory consolidation could not be always in an excitation state, rebound inhibition may be expected following an activity burst as some previous electrophysiological data had shown (40). It is also likely that a prolonged inhibition state arises right after a learning event, then the brain activity gradually turn back to the baseline by increasing excitatory activity (30, unpublished data). No matter the persistent depression is induced by post-activation suppression or initially set off during consolidation, it may result in greater reduction of Mn^{2+} uptake in the IA group comparing with the CC group, because the latter group may accumulate mild spontaneous activation over the 24 h without engaging any deep depression. Finally, depression may

also be caused by norepinephrine, a neurotransmitter often released to enable memory consolidation (34); it acts by increasing the firing threshold and thus enhancing the signal to noise ratio for the learned stimulus. Its release during consolidation may associate with an overall reduction of neural activity. If these conjectures are indeed the case, then sampling Mn^{2+}-enhanced imaging at different times rather than adding all post-training activities over a 24-h period may yield different patterns of activity mapping.

In either voxel by voxel analysis or ROI analysis, the present study found signal difference between the IA and CC groups in the medial prefrontal cortex including the prelimbic and Cg areas, insular cortex and anterior piriform cortex. The changes of Mn^{2+} signals in these regions may be related to the nature of inhibitory avoidance memory. This task contains in essence both classical and operant conditioning, the former type of learning allows the rat to associate the aversive shock to spatial or contextual cues of the apparatus, while the latter inhibits approaching behavior to the darkness contingent upon previous punishment (24). The medial prefrontal cortex is implicated in fear conditioning for it receives converging inputs from the hippocampus transacting spatial cues and from the amygdala transacting emotional cues. Blocking this region impaired consolidation of long-term memory and retrieval of remote memory in the inhibitory avoidance task (24, 25). These data supports the present results suggesting that neural plasticity residing in the medial prefrontal region, possibly the prelimbic and Cg areas, is involved in consolidation of inhibitory avoidance memory.

Likewise, the insular cortex has also been implicated in various forms of aversive learning including the inhibitory avoidance task (3, 26). The insular cortex receives visceral input ascending from the periphery and neurons therein could be activated by nociceptive stimuli applied to the limb (42), thus this area may be engaged by aversive visceral and somatic input due to the training shock to join the neural circuitry of memory consolidation. The anterior piriform cortex traditionally was viewed to process olfactory cues and little evidence has shown a role of this area in the IA task. Thus, the present study provides the first piece of evidence suggesting involvement of the anterior piriform cortex in IA memory processing. The olfactory cues in the IA task were not contingent upon shock administration, yet it may provide some background information to form a context representation, which is critical for acquiring a fear response to a context such as the IA apparatus (8). In view of the critical role of operant conditioning in the IA task (24), one would expect participation of the nucleus accumbens as it is the sole neural substrate interfacing aversive motivation to motor acts (35). However, this study failed to detect a significant change in Mn^{2+} signals in this region, although it showed the largest non-significant reduction in our data set. This area should be better pursued in the future.

The most significant finding of the present study is that a network with selective, refined functional connectivity emerged from a set of brain regions which were non-discriminatively related in the control state. The results hint that the cell assembly underlying long-term memory is formed within the brain by pruning the unneeded functional connectivity instead of strengthening the needed one. This way of action is well consistent with the tenet of neural Darwinism raised to account for plasticity in neural development (15). As a matter of fact, by adopting the same graphing method in analyzing brain activity signal inferred from blood flow, Wang and colleagues also found fewer connections and more concentrated clusters in the functional network during recall of an inhibitory avoidance response motivated by visceral pain (47). Accordingly in a human fMRI study, Payne and Kensinger (39) found a night of sleep for memory consolidation can lead to a shift from engaging a diffused memory retrieval network to become a more refine, efficient one, including the amygdala and ventromedial prefrontal cortex. These results suggested that a well consolidated memory relied on a more concentrated functional network with less direct communication among nodes.

How the functional connectivity detected in the present study relates to the actual connections is not completely clear. For example, reciprocal communication between the prelimbic region and amygdala is anatomically present (1, 7), and behavioral studies have shown interaction between these two regions in memory consolidation (25). Yet, in Fig. 3B, functional connectivity between the amygdala and prelimbic area inferred from MEMRI requires 4 link steps (*via* ventral hippocampus, anterior cingulate cortex, nucleus accumbens) to mutually connect. How these structures in mediating the interaction between the prelimbic area and amygdala are unclear, but the findings suggest that the interaction between these two areas may further be modulated by inputs from the intervening regions during consolidation. However, it should be noted that once memory was well consolidated and could be readily retrieved during a retention test, the prelimbic area may directly communicate with other brain regions as shown by Wang and colleagues (47).

It is also intriguing that three clusters emerged in the consolidation period: The anterior piriform, insular, prelimbic, and anterior cingulate cortices, ventral subiculum, lateral septum, and nucleus accumbens showed highly inter-correlated Mn^{2+} signals;

the S1, BNST and caudate-putamen formed another group with high inter-correlated activity; and finally the dorsal and ventral hippocampus, amygdala, and thalamus formed a loop serving to bridge the former two. The functional significance of these three clusters can only be conjectured. The first cluster containing the cortices as well as some subcortical structures sensitive to internal or external states may process the internal milieu or external context. In the second cluster, the caudate-putamen complex may mediate the avoidance behavior and the BNST may mediate various autonomic and hormonal responses accompanying with that behavior. Finally, the third cluster of an amygdala-hippocampus-thalamus loop serves as a kernel to bind all information together. This conjecture should be experimentally examined in future studies.

It should be noted that the present activation pattern and functional connectivity reflect an offline memory process in the brain at the time when no learning-related input and output prevail. Therefore these results are not comparable to what have been reported in several other studies which focused on retrieving well-consolidated memory, in which the activity pattern reflects online processing of memory stored in the brain regions (14, 23). Consistent with such data, our laboratory has shown that by mapping Fos expression, the functional network during retrieving 1-day IA memory also had distinct clusters showing activity correlation that was high within a cluster but low between clusters (50); yet brain regions of the trained group including the prelimbic area and nucleus accumbens showed increased activity during retrieval, which was also well correlated with retention performance. It is very intriguing why a brain region in the same cell assembly subserving a memory trace had opposite responses in the consolidation and retrieval phases, and this question should be pursued in the future.

In conclusion, the present study used MEMRI to detect functional change of the whole brain within 24 h after training, which covered the critical period of memory consolidation. It found a significant reduction of Mn^{2+} signals in the prelimbic, insular and anterior piriform cortices. Further, inter-regional functional connectivity based on correlation analysis of Mn^{2+} signals across regions detected confinement rather than expansion of communication within a brain network. These results suggest that a long-term memory trace may be laid down by pruning exuberant neural connectivity in a cell assembly.

Acknowledgments

We thank 7T animal MRI Core Lab of the Neurobiology and Cognitive Science Center, National Taiwan University for technical and facility supports. This study was supported by grants NSC 98-2410-H-002-024-MY3, NSC 101-2410-H-002-082-MY3 from the National Science Council and Aim for Top University Excellent Research Project 10R80918/101R8921 from Ministry of Education, Taiwan, ROC.

References

1. Bacon, S.J., Headlam, A.J., Gabbott, P.L. and Smith, A.D. Amygdala input to medial prefrontal cortex (mPFC) in the rat: a light and electron microscope study. *Brain Res*. 720: 211-219, 1996.
2. Batagelj, V. and Mrvar, A. Pajek-Analysis and Visualization of Large Networks. In: *Graph Drawing Software*, edited by Jünger, M. and Mutzel, P. Berlin: Springer, 2004, pp. 77-103.
3. Bermudez-Rattoni, F., Introini-Collison, I.B. and McGaugh, J.L. Reversible inactivation of the insular cortex by tetrodotoxin produces retrograde and anterograde amnesia for inhibitory avoidance and spatial learning. *Proc. Natl. Acad. Sci. USA* 88: 5379-5382, 1991.
4. Buckner, R.L. and Vincent, J.L. Unrest at rest: Default activity and spontaneous network correlations. *Neuroimage* 37: 1091-1096, 2007.
5. Bullmore, E. and Sporns, O. Complex brain networks: graph theoretical analysis of structural and functional systems. *Nat. Rev. Neurosci.* 10: 186-198, 2009.
6. Carr, M.F., Jadhav, S.P. and Frank, L.M. Hippocampal replay in the awake state: a potential substrate for memory consolidation and retrieval. *Nat. Neurosci*. 14: 147-153, 2011.
7. Cassell, M.D. and Wright, D.J. Topography of projections from the medial prefrontal cortex to the amygdala in the rat. *Brain Res. Bull*. 17: 321-333, 1986.
8. Chang, S.D., Chen, D.Y. and Liang, K.C. Infusion of lidocaine into the dorsal hippocampus before or after the shock training phase impaired conditioned freezing in a two-phase training task of contextual fear conditioning. *Neurobiol. Learn. Mem*. 89: 95-105, 2008.
9. Chen, W., Tenney, J., Kulkarni, P. and King, J.A. Imaging unconditioned fear response with manganese-enhanced MRI (MEMRI). *Neuroimage* 37: 221-229, 2007.
10. Chuang, K.H., Lee, J.H., Silva, A.C., Belluscio, L. and Koretsky, A.P. Manganese enhanced MRI reveals functional circuitry in response to odorant stimuli. *Neuroimage* 44: 363-372, 2009.
11. Cox, R.W. AFNI: software for analysis and visualization of functional magnetic resonance neuroimages. *Comput. Biomed. Res*. 29: 162-173, 1996.
12. Diekelmann, S., Buchel, C., Born, J. and Rasch, B. Labile or stable: opposing consequences for memory when reactivated during waking and sleep. *Nat. Neurosci*. 14: 381-386, 2011.
13. Dudai, Y. The Restless Engram: Consolidations Never End. *Annu. Rev. Neurosci*. 35: 227-247, 2012.
14. Durrant, S.J., Cairney, S.A. and Lewis, P.A. Overnight consolidation aids the transfer of statistical knowledge from the medial temporal lobe to the striatum. *Cereb. Cortex*, advance online publication, doi: 10.1093/cercor/bhs244, 2012.
15. Edelman, G.M. *Neural Darwinism: the theory of neuronal group selection*. New York: Basic Books, 1987.
16. Eschenko, O., Canals, S., Simanova, I., Beyerlein, M., Murayama, Y. and Logothetis, N.K. Mapping of functional brain activity in freely behaving rats during voluntary running using manganese-enhanced MRI: Implication for longitudinal studies. *Neuroimage* 49: 2544-2555, 2010.
17. Gupta, A.S., van der Meer, M.A.A., Touretzky, D.S. and Redish, D.A. Hippocampal replay is not a simple function of experience. *Neuron* 65: 695-705, 2010.

18. Hebb, D.O. *The Organization of Behavior: A Neuropsychological Theory*. New York: John Wiley and Sons, 1949.
19. Inui, T., Inui-Yamamoto, C., Yoshioka, Y., Ohzawa, I. and Shimura, T. Activation of projective neurons from the nucleus accumbens to ventral pallidum by a learned aversive taste stimulus in rats: a manganese-enhanced magnetic resonance imaging study. *Neuroscience* 177: 66-73, 2011.
20. Laurent, V. and Westbrook, R.F. Inactivation of the infralimbic but not the prelimbic cortex impairs consolidation and retrieval of fear extinction. *Learn. Mem*. 16: 520-529, 2009.
21. Lee, E.H.Y., Lin, W.R., Chen, H.Y., Shiu, W.H. and Liang, K.C. Fluoxetine and 8-OH-DPAT in the lateral septum enhances and impairs retention of an inhibitory avoidance response in rats. *Physiol. Behav*. 51: 681-688, 1992.
22. Lewis, C.M., Baldassarre, A., Committeri, G., Romani, G.L. and Corbetta, M. Learning sculpts the spontaneous activity of the resting human brain. *Proc. Natl. Acad. Sci. USA* 106: 17558-17563, 2009.
23. Lewis, P.A., Cairney, S., Manning, I. and Critchley, H. The impact of overnight consolidation upon memory for emotional and neutral encoding contexts. *Neuropsyhologia* 49: 2619-2629, 2012.
24. Liang, K.C. Involvement of the amygdala and its connected structures in formation and expression of inhibitory avoidance memory: issues and implications. *Chinese J. Physiol*. 52: 196-214, 2009.
25. Liang, K.C., Hu, S.J. and Chang, S.C. Formation and retrieval of inhibitory avoidance memory: differential roles of glutamate receptors in the amygdala and medial prefrontal cortex. *Chinese J. Physiol*. 39: 155-166, 1996.
26. Liang, K.C. and Liao, W.L. Pretest infusion of lidocaine into the insular or medial prefrontal cortex impairs retrieval of remote memory in an inhibitory avoidance task. *Soc. Neurosci, Abst*. 21: 1448, 1995.
27. Liang, K.C., Melia, K.R., Campeau, S., Falls, W.A., Miserendino, M.J. and Davis, M. Lesions of the central nucleus of the amygdala, but not the paraventricular nucleus of the hypothalamus, block the excitatory effects of corticotropin-releasing factor on the acoustic startle reflex. *J. Neurosci*. 12: 2313-2320, 1992.
28. Liu, C.H., D'Arceuil, H.E. and de Crespigny, A.J. Direct CSF injection of MnCl2 for dynamic manganese-enhanced MRI. *Magn. Reson. Med*. 51: 978-987, 2004.
29. Liu, T.L. and Liang, K.C. Posttraining infusion of cholinergic drugs into the ventral subiculum modulated memory in an inhibitory avoidance task: interaction with the bed nucleus of the stria terminalis. *Neurobiol. Learn. Mem*. 91: 235-242, 2009.
30. Liu, T.L. and Liang, K.C. Rol*e and interaction between the bed nucleus of stria terminalis and the ventral subiculum on fear memory formation*. Unpublished doctoral dissertation, National Taiwan University, Taipei, Taiwan, 2013.
31. Lu, H., Xi, Z.X., Gitajn, L., Rea, W., Yang, Y. and Stein, E.A. Cocaine-induced brain activation detected by dynamic manganese-enhanced magnetic resonance imaging (MEMRI). *Proc. Natl. Acad. Sci. USA* 104: 2489-2494, 2007.
32. McGaugh, J.L. Memory — a century of consolidation. *Science* 248: 248-251, 2000.
33. McGaugh, J.L. The amygdala modulates the consolidation of memories of emotionally arousing experiences. *Annu. Rev. Neurosci*. 27: 1-28, 2004.
34. McIntyre, C.K., Hatfield, T. and McGaugh, J.L. Amygdala norepinephrine levels after training predict inhibitory avoidance retention performance in rats. *Eur. J. Neurosci*. 16: 1223-1226, 2002.
35. Mogenson, G.J., Jones, D.L. and Yim, C.Y. From motivation to action: functional interface between the limbic system and the motor system. *Prog. Neurobiol*. 14: 69-97, 1980.
36. Pautler, R.G. *In vivo*, trans-synaptic tract-tracing utilizing manganese-enhanced magnetic resonance imaging (MEMRI). *NMR Biomed*. 17: 595-601, 2004.
37. Pautler, R.G. and Koretsky, A.P. Tracing odor-induced activation in the olfactory bulbs of mice using manganese-enhanced magnetic resonance imaging. *Neuroimage* 16: 441-448, 2002.
38. Paxinos, G. and Watson, C. *The Rat Brain in Stereotaxic Coordinates*. 5th ed. Elsevier Academic Press, 2005.
39. Payne, J.D. and Kensinger, E.A. Sleep leads to changes in the emotional memory trace: evidence from fMRI. *J. Cognitive Neurosci*. 23: 1285-1297, 2011.
40. Pelletier J.G., Likhtik, E., Filali, M. and Pare, D. Lasting increases in basolateral amygdala activity after emotional arousal: Implications for facilitated consolidation of emotional memories. *Learn. Mem*. 12: 96-102, 2005.
41. Quirk, G.J., Likhtik, E., Pelletier, J.G. and Paré, D. Stimulation of medial prefrontal cortex decreases the responsiveness of central amygdala output neurons. *J. Neurosci*. 23: 8800-8807, 2003.
42. Shih, Y.Y., Chang, C., Chen, J.C. and Jaw, F.S. BOLD fMRI mapping of brain responses to nociceptive stimuli in rats under ketamine anesthesia. *Med. Eng. Phys*. 30: 953-958, 2008.
43. Silva, A.C., Lee, J.H., Aoki, I. and Koretsky, A.P. Manganese-enhanced magnetic resonance imaging (MEMRI): methodological and practical considerations. *NMR Biomed*. 17: 532-543, 2004.
44. Tambini, A., Ketz, N. and Davachi, L. Enhanced brain correlations during rest are related to memory for recent experiences. *Neuron* 65: 280-290, 2010.
45. Valverde, F. Reticular formation of the albino rat's brain stem cytoarchitecture and corticofugal connections. *J. Comp. Neurol*. 119: 25-53, 1962.
46. Van der Linden, A., Verhoye, M., van Meir, V., Tindemans, I., Eens, M., Absil, P. and Balthazart, J. *In vivo* manganese-enhanced magnetic resonance imaging reveals connections and functional properties of the songbird vocal control system. *Neuroscience* 112: 467-474, 2002.
47. Wang, Z., Bradesi, S., Charles, J.R., Pang, R.D., Maarek, J.M., Mayer, E.A. and Holschneider, D.P. Functional brain activation during retrieval of visceral pain-conditioned passive avoidance in the rat. *Pain* 152: 2746-2756, 2011.
48. Weng, J.C., Chen, J.H., Yang, P.F. and Tseng, W.Y.I. Functional mapping of rat barrel activation following whisker stimulation using activity-induced manganese-dependent contrast. *Neuroimage* 36: 1179-1188, 2007.
49. Yang, P.F., Chen, D.Y., Hu, J.W., Chen, J.H. and Yen, C.T. Functional tracing of medial nociceptive pathways using activity-dependent manganese-enhanced MRI. *Pain* 152: 194-203, 2011.
50. Yang, Y.P. and Liang, K.C. Region specific c-Fos expression in formation and expression of inhibitory avoidance memory. *Soc. Neurosci, Abst*. 42: 2663, 2012.
51. Yu, X., Wadghiri, Y.Z., Sanes, D.H. and Turnbull, D.H. *In vivo* auditory brain mapping in mice with Mn-enhanced MRI. *Nat. Neurosci*. 8: 961-968, 2005.